Material Properties of the Human Cranial Vault and Zygoma

JILL PETERSON[1] AND PAUL C. DECHOW[2]*
[1]Department of Public Health, Baylor College of Dentistry, Texas A & M University System Health Science Center, Dallas, Texas
[2]Department of Biomedical Sciences, Baylor College of Dentistry, Texas A & M University System Health Science Center, Dallas, Texas

ABSTRACT

The material properties of cortical bone from the diaphyses of long bones (e.g., the femur and tibia) vary by direction, such that bone is stiffer and stronger along its long axis. This configuration improves the abilities of these structures to resist axial compressive loads coupled with bending. As in long bones, cortical bone from the cranial vault is subject to mechanical loads from various orofacial functions and the contraction of attached muscles. However, experimental studies suggest that the resulting bone strains are at least an order of magnitude smaller than those found in the midshafts of the femur or tibia. The characteristics of the three-dimensional elastic properties of cortical bone are largely unexplored in regions of low bone strain, including the cranial vault, in which little is known regarding cortical structure and function. In the present study we examined variations in the cortical microstructure and material properties of the bone of the human cranial vault, including the parietal, frontal, temporal, and occipital bones. A facial bone, the zygoma, was also included to contrast the properties of the cranial vault with another craniofacial intramembranous bone that experiences larger strains. Cortical specimens from the outer cortical plate of the cranial vault were removed from 15 frozen human crania. We measured cortical thicknesses and densities, and determined the primary direction of stiffness within the bone specimens prior to ultrasonic testing to determine their elastic properties. There were statistically significant differences in elastic properties between bones and, in some cases, sites within bones, which for most variables were clustered by bone or region. In striking contrast to this pattern, elastic moduli in the direction of primary stiffness were larger in cortical regions underlying muscle attachments than in regions without muscle attachments. Few sites in the cranial vault or zygoma showed a consistent orientation of the material axes among individuals, although specimens from many regions had directional differences similar to those in cortical bone from the mandible, femur, or tibia. Anat Rec Part A 274A:785–797, 2003.

Key words: biomechanics; skeletal function; craniofacial biology; bone adaptation; microstructure

Although the cranial vault serves various important functions, such as providing an attachment for the orofacial musculature and protecting the brain, the variability in its structural and mechanical characteristics has been largely uninvestigated. The human cranial vault is comprised of the frontal, parietal, occipital, sphenoid, and temporal bones. Each consists entirely or partially of diploic bone, which is constructed of two cortical plates sandwiching a layer of trabecular bone (Sicher and DuBrul, 1970).

Locally, the cranial vault may bear significant loads in those portions that serve as anchorage for masticatory and nuchal musculature (Behrents et al., 1978). However, results from in vitro studies in humans (Endo, 1966, 1970) and in vivo studies in other mammals (Hylander, 1987), especially in the region of the upper face and brow ridges,

Grant sponsor: NIH NIDCR; Grant number: K08 DE00403.
*Correspondence to: Dr. Paul C. Dechow, Department of Biomedical Sciences, Baylor College of Dentistry, 3302 Gaston Ave., Dallas, TX 75246. Fax: (214) 828-8951.
E-mail: pdechow@tambcd.edu
Received 3 July 2002; Accepted 3 April 2003
DOI 10.1002/ar.a.10096

suggest that at least portions of the human cranial vault endure very low strains during biting or mastication, compared to the mandible and postcranial long bones. These findings led to the suggestion that the cranial vault is overbuilt for the function of resisting stresses generated by craniofacial functions and muscular contractions (Ravosa et al., 2000).

The role of mechanical stimuli in the maintenance of cortical bone structure in the cranial vault is unknown. The low strains suggest that 1) mechanical loading is less important than in other parts of the skeleton for maintaining skeletal mass and form, 2) lower thresholds of strain in the cranial vault are necessary for skeletal maintenance, or 3) some combination of these factors may occur. It is clear that mechanical influences do influence the structure of the cortical bone of the cranial vault. However, aside from anatomical descriptions of the ridges and processes associated with muscle attachment, and the mechanical properties of the full-thickness diploic bone (Evans and Lissner, 1957; Schröder et al., 1977), there has been little exploration of the variability in the mechanical characteristics of cranial cortical bone, or of how it compares to cortical bone from more highly strained regions. A detailed examination of this variability, and a comparison with cortical bone from elsewhere in the skeleton, may shed considerable light on the adaptive potential of cranial cortical bone, and provide clues as to how function influences its intermediate structure.

The sparse data on the material properties and related micromechanical features of cranial cortical bone are limited by a lack of knowledge concerning its unique three-dimensional properties. This problem can be clarified by considering the cortical structure in the postcranial skeleton. The mechanical properties of the cortex in the diaphyses of long bones are typically characterized along three axes, including the anatomical longitudinal axis, which is considered to be the axis of maximum stiffness. At right angles to the longitudinal axis are 1) the circumferential axis, which is tangential to the cortical surface; and 2) the radial axis, which is perpendicular to the plane of the cortical plate, and is the axis in which cortical thickness is measured. It is well known that diaphyseal cortical bone can be described as anisotropic (or, more specifically, orthotropic) because its elastic properties differ along these three axes, with the bone being stiffest in the longitudinal direction. Remodeled bone is often described as transversely isotropic because elastic properties are similar along the circumferential and tangential axes, while bone in the longitudinal direction is stiffer.

In cranial bone, the axes within the plane of the cortical plate cannot be determined by anatomical landmarks, as we have shown in the mandible (Schwartz-Dabney and Dechow, 2003). In other bones of the cranium, such as the parietal bone (Peterson and Dechow, 2002), it is even less clear what anatomical landmarks might correspond with the material axes of cortical bone from various regions. The idea that grain in cortical bone, or the direction of maximum stiffness, aligns in the direction of maximum stress may be a reasonable conjecture on which to base hypotheses about directions of maximum stiffness. However, it is difficult to test this conjecture, especially in bones that are likely to have complex loading patterns (such as the cranial vault, in which little is known about loading patterns).

Results from structural studies of the parietal bone (Peterson and Dechow, 2002) indicate that cortical bone from both the periosteal and endosteal surfaces exhibit at least some degree of anisotropy (differences in elastic properties by direction), and some regions have consistent orientations of the axis of maximum stiffness. These findings contrast with those from an earlier study (Dechow et al., 1993), which suggested that supraorbital cortical bone has similar elastic properties (isotropy) in directions that parallel the plane of the cortical plate. However, in the earlier study it was assumed that the direction of maximum stiffness would not vary significantly between individuals, and therefore such differences were not explored. The finding of isotropy in the plane of the cortical plate was derived from the lack of statistically significant differences in mean longitudinal ultrasonic velocity in three directions based on anatomical position. The orientation of maximum longitudinal ultrasonic velocity, which coincides with the direction of peak stiffness, was not determined in each bone sample prior to the calculation of elastic properties.

Our goal in the present work was to explore the variability in the mechanical properties of the periosteal cortex of the cranial vault bones. We hypothesized that there are differences between cranial vault skull bones and between regions within individual bones that correspond with variations in function and development. In this study we also included samples of cortical bone from the zygoma. Because the zygoma is a facial bone, it is interesting to compare it with the adjacent temporal and frontal bones, as it participates in common support functions (although it experiences greater levels of strain) and does not directly contribute to the protection of the brain.

MATERIALS AND METHODS

We used bone specimens removed from 15 dentate (i.e., all teeth present, excluding third molars) human crania selected from unembalmed, fresh-frozen, whole cadaver heads. Fifteen subjects (Caucasian, seven females and eight males, 27–100 years old, mean age 68.4 years), in a random mix, were studied. Specimens were not collected from persons known to have died from primary bone diseases. The crania were stored in freezers at –10°C prior to removal of bone specimens. It has been found that the freezing process has a minimal effect on the elastic properties of bone (Dechow and Huynh, 1994; Evans, 1973; Zioupos et al., 2000).

Cylindrical cortical bone specimens (4 mm in diameter) were harvested from the zygomatic (four sites), frontal (nine sites), occipital (five sites), parietal (14 sites), and temporal (four sites) bones (Fig. 1). Sites for bone sampling were selected to provide an overview of elastic properties of cortical bone from throughout the outer table of the cranium, and, in particular, a representative sample from each cranial bone.

Bone preparation and testing procedures were similar to those previously described (Peterson and Dechow, 2002; Schwartz-Dabney and Dechow, 2003). Universal precautions for infection control were used during all bone-preparation procedures. We removed each bone sample with a dental handpiece using a 4.0 ID trephine burr (5.0 mm OD; Nobelpharma, Göteborg, Sweden). The samples were continuously cooled with a water drip during preparation. Prior to removal, each bone sample was marked with a graphite line that paralleled the sagittal suture, indicat-

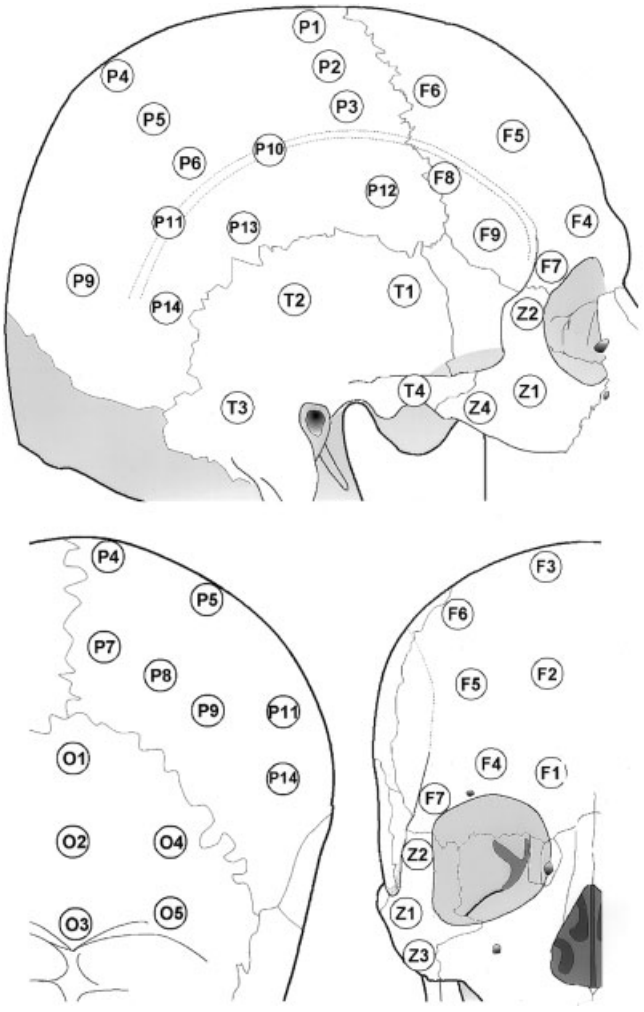

Fig. 1. Location of sites on the parietal, frontal, temporal, occipital, and zygomatic bones in three views. Each site is numbered for reference.

ing the sample's orientation. The rostral and anterior ends of the line were marked with an arrowhead to indicate direction.

After the bone core was removed, the diploë (or residual trabecular bone) was removed by grinding with a miniature lathe (Unimat 3, Emco, Austria) under water irrigation, while preserving the outer cortical plate. The samples were stored in a solution of 95% ethanol and isotonic saline in equal proportions. This media maintains the elastic properties of cortical bone over time, with minimal change (Ashman et al., 1984; Dechow and Huynh, 1994).

We measured the cortical thickness of each bone specimen. We then calculated the apparent density from the sample weight and differential volume in water based on Archimedes' principle of buoyancy (Ashman et al., 1984). Each sample was measured at least twice to ensure the reliability of the density measurements. If densities differed between trials, the measurements were repeated until consistent results were obtained.

Before the elastic properties of each specimen are measured, it is essential to determine the axes of maximum (d_3) and minimum (d_2) stiffness within the plane of the cortical plate, as these axes do not necessarily coincide with anatomical features in the cranial skeleton. To accomplish this, we used a modification of previous techniques (Ashman, 1982; Ashman et al., 1984; Ashman and Van Buskirk, 1987), in that cylindrical specimens were used (Schwartz-Dabney and Dechow, 2002, 2003).

In cylindrical specimens, the axes are determined experimentally by passing longitudinal ultrasonic waves generated by 2.25 MHz piezoelectric transducers (V323-SU; Panametrics, Waltham, MA) through each cortical specimen in nine directions with 22.5° intervals. As on a clock face, we aligned our orientation line and arrow, which was drawn on each specimen prior to bone core removal, in the direction of 12:00 (direction 1). Directions 1 and 9 (6:00 on the clock face) were identical and served as an internal control, because the ultrasonic velocities in those two directions should be equal. Directions 1 and 9 were 180° apart, and in our bidirectional system represented the same orientation, but with the emitting and receiving ultrasonic transducers reversed in position. The resulting time delay corresponded to the propagation of the wave through the thickness of the specimen plus the system delay, and it measured a phase comparison of the signal before and after its transmission. Ultrasonic velocities were then calculated taking into account the time delay, system delay, and thickness of the specimen.

The direction of the axis of maximum stiffness (d_3) corresponded with the direction of peak longitudinal ultrasonic velocity. As velocity measurements were made at 22.5° intervals around half the circumference of each specimen, the direction of the axis of maximum stiffness was determined to within 11.25°. Perpendicular to the axis of maximum stiffness within the plane of the cortical plate was the axis of minimum stiffness, or d_2. Ultrasonic waves along this axis had the lowest velocity within that plane.

The elastic constants were calculated as previously described (Ashman, 1982; Ashman et al., 1984; Ashman and Van Buskirk, 1987), which required the measurement of additional ultrasonic velocities, including longitudinal velocities through the thickness of the cortex, and a series of transverse wave velocities. The latter velocities were measured with 5.0 MHz transducers (V156-RM; Panametrics, Waltham, MA) along the three major axes (d_1, d_2, and d_3) and in several off-axis orientations (Ashman et al., 1984).

Relationships between the various velocities through the specimen and its material properties were derived from the principles of linear elastic wave theory, based on Hooke's law, according to the technique of Ashman et al. (1984). The calculated elastic constants included: 1) the elastic modulus (a measure of the ability of a structure to resist deformation in a given direction), 2) the shear modulus (a measure of the ability of a structure to resist shear stresses), and 3) the Poisson's ratio (a measure of the ability of a structure to resist deformation perpendicular to that of the applied load).

Data were analyzed using the Minitab statistical analysis program (Minitab, Inc., State College, PA). Descriptive statistics, including means, standard deviations (SDs), and standard errors, were calculated for all measurements. Correlation coefficients were also calculated to examine the relationships between selected variables.

The assessment of differences between bones and between sites within bones was restricted by the lack of independence between multiple samples taken from a sin-

gle specimen. Testing for differences thus required the use of an analysis of variance (ANOVA) with a repeated-measures design to account for the lack of independence (Schwartz-Dabney and Dechow, 2003). We used a balanced, unrestricted ANOVA with a repeated-measures design and subject as the random factor to test for overall differences in density, cortical thickness, and elastic properties. Sites were clustered by bone, resulting in tests for significant differences between bones, and between sites within bones.

Because of the large number of possible individual comparisons, post hoc tests were not generated for all combinations of sites. If significant differences were found in the overall ANOVA, we made post hoc comparisons by plotting and comparing means and 95% confidence intervals (CIs). Our findings describe the largest differences between bones and sites within bones, and exclude results where there was overlap of the CIs.

A second data grouping was used to compare muscle-bearing and non-muscle-bearing bone. Muscle-bearing sites included regions of attachment for the temporalis (P10, P11, P12, P13, P14, T1, T2, F8, and F9), masseter (T4 and Z4), and nuchal musculature (O2, O3, O4, and O5). We again used a balanced, unrestricted ANOVA with a repeated-measures design and subject as the random factor to account for the lack of independence between bone specimens from a single individual skull. The analyses differed in that data were not clustered by bone. Rather, we tested for an overall differences between muscle-bearing and non-muscle-bearing sites in density, cortical thickness, and elastic properties.

Angular measurements (orientation of maximum stiffness) were analyzed with circular descriptive statistics, including the mean vector, circular SD, standard error, CI, and Rayleigh's test of uniformity (Fisher, 1993), with the Oriana Statistical Analysis Program (Kovach Computing Services; Anglesey, Wales, UK). The Rayleigh's test of uniformity revealed whether a site actually had a significant mean angle (oriented site) or whether the distribution of angles between individuals could not be distinguished from a random distribution (non-oriented site). If a site had a statistically significant interindividual orientation, then a generalized version of the Watson-Williams test determined differences between circular means across sites.

We also tested whether muscle-bearing bone had a higher number of sites that were significantly oriented as determined by the Rayleigh's test of uniformity. A 2×2 chi-square test was used to determine whether there was a difference between muscle-bearing bone and non-muscle-bearing bone in the number of oriented and nonoriented sites.

TABLE 1. Density (g/cm^3), cortical thickness (mm)

		Density		Thickness	
Bone	Site	Mean	SD	Mean	SD
Parietal	1	1.877	.092	2.8	0.9
	2	1.845	.122	2.6	0.7
	3	1.795	.153	2.7	0.6
	4	1.803	.098	2.9	0.7
	5	1.772	.128	2.8	0.7
	6	1.766	.119	2.5	0.6
	7	1.825	.111	2.8	0.6
	8	1.773	.086	2.4	0.7
	9	1.807	.098	2.4	0.6
	10	1.779	.129	2.5	0.5
	11	1.813	.148	2.5	0.7
	12	1.824	.173	2.4	0.6
	13	1.859	.136	2.4	0.6
	14	1.841	.164	2.2	0.7
Grand mean		1.812	.127	2.5	0.7
Frontal	1	1.780	.095	2.5	0.4
	2	1.788	.117	2.6	0.3
	3	1.828	.128	2.4	0.7
	4	1.784	.128	2.4	0.5
	5	1.771	.116	2.7	0.6
	6	1.818	.126	2.4	0.5
	7	1.744	.131	2.4	0.5
	8	1.760	.153	2.6	0.8
	9	1.767	.153	2.6	0.6
Grand mean		1.783	.128	2.5	0.5
Occipital	1	1.786	.139	3.1	0.4
	2	1.816	.170	3.3	1.1
	3	1.911	.091	2.9	1.4
	4	1.878	.104	2.7	0.6
	5	1.907	.117	3.0	0.9
Grand mean		1.860	.133	3.0	0.9
Temporal	1	1.803	.190	1.8	0.4
	2	1.859	.158	1.8	0.4
	3	1.922	.098	3.1	1.0
	4	1.899	.111	2.4	0.4
Grand mean		1.868	.149	2.3	0.8
Zygoma	1	1.686	.216	2.1	0.5
	2	1.758	.192	2.3	0.5
	3	1.615	.165	2.2	0.4
	4	1.654	.200	2.0	0.6
Grand mean		1.679	.197	2.2	0.5
Grand mean	MBB[a]	1.800	.166	2.4	0.8
Grand mean	Non-MBB	1.806	.124	2.6	0.6
ANOVA		F	P	F	P
Bones		13.8	0.001	10.4	0.001
Site/bone		3.2	0.001	2.8	0.001
Muscle	MB	0.3	NS	12.4	0.003

[a]MBB, muscle bearing bone.

RESULTS

There were significant differences in density between bones and sites within bones (Table 1). The average density by site ranged from 1.615 g/cm^3 to 1.922 g/cm^3. The temporal bone was the most dense, with a grand mean of 1.868 g/cm^3, and the zygoma was the least dense, with a grand mean of 1.679 g/cm^3. The site on the temporal bone, next to the occipitomastoid suture (T3), was the densest site (1.922 g/cm^3). Most differences within bones were small compared to differences between bones, with a few exceptions. Within the temporal bone, T1 resembled adjacent sites in the frontal bone more than the other temporal bone sites. Within the zygoma, Z2 resembled the adjacent frontal bone site F7 and other cranial vault sites more than it resembled Z3.

Significant differences were observed in the thickness of the external cortical plate between bones and between sites within bones (Table 1). The external cortex was thickest within the occipital bone, averaging a grand mean of 3.0 mm across five sites, and at site T3, which was the most posterior site on the temporal bone bordering the occipital bone (3.1 mm) and was much thicker than other temporal bone sites. The site superior to the external occipital protuberance (O2) was the thickest of any site (3.3 mm). The cortical bone was thinnest in the squamous portion of the temporal bone (sites T1 and T2), averaging

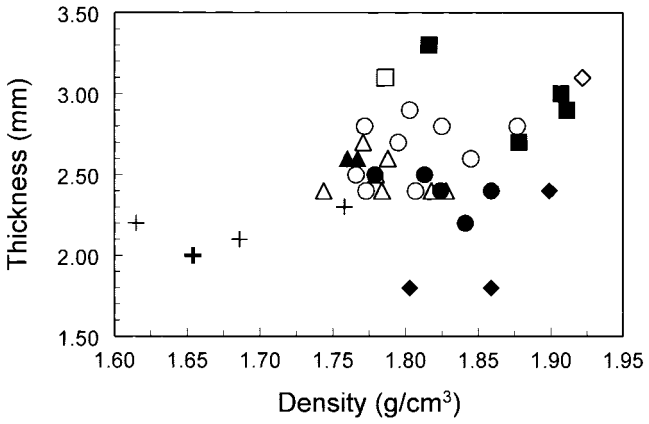

Fig. 2. Scatterplot of mean thickness vs. mean density by site. Solid shapes indicate muscle-bearing (M) sites, and hollow shapes are non-muscle-bearing (NM) sites. Squares: occipital bone sites; diamonds: temporal bone sites; pluses: zygomatic bone sites; circles: parietal bone sites; triangle: frontal bone sites.

1.8 mm. Within the parietal bone, the thickest site, P4 (2.9 mm), at the parietal boss was much thicker than the thinnest parietal bone site, P14 (2.2 mm), which was more similar to the adjacent temporal bone site, T2 (1.8 mm).

Thickness and density are both major factors in the structural mechanics of cortical bone, but they were not significantly correlated in our sample. Figure 2 shows a plot of mean thicknesses and densities by site clustering the data by bone, illustrating regional similarities. Sites from the parietal and frontal bones were clustered together. Sites from the zygoma had lower values of density than sites from the cranial vault bones, except for site Z2, which resembled the adjacent frontal bone site. In thickness, the zygoma was in the lower range of values, but it overlapped with sites from the temporal and parietal bones. Sites from the occipital bone were slightly thicker and denser than those from the parietal and frontal bones. Sites from the temporal bone were thinner but similar in density to those of the frontal and parietal bones, except for site T3, the site on the temporal bone next to the occipitomastoid suture, which was similar in the average of its properties to sites on occipital bone.

The values for elastic moduli demonstrated differences by direction, in that E_3 was larger than E_2, which was larger than E_1. When elastic moduli were analyzed separately, each showed significant differences between bones and between sites within bones.

Between bones, there were different patterns for E_1 and E_2 compared to E_3. This pattern was similar to that described above for variations in thickness. For E_1 and E_2, the largest difference was that the zygoma, a facial bone, had smaller moduli. Within the cranial vault, E_1 had the lowest values of all directions, varying from 11.7 GPa (T1) to 15.0 GPa (T3). Sites on the zygoma differed, as all means averaged $<$10.5 GPa. On the cranial vault, E_2 varied from 10.5 GPa (Z4) to 17.7 GPa (T3), while all sites within the zygoma had values of $<$11.7 GPa. Other consistent, but smaller, differences were also apparent. Values from the occipital bone were among the largest for E_1 and E_2, respectively. The parietal and frontal bones had more intermediate values, while the temporal bone had a greater range of variability, especially for E_2.

Means of E_3 varied from 17.6 GPa (F9) to 27.3 GPa (T3), and showed greater variance within each bone and less variance between bones than did E_1 or E_2. Overall, means from the occipital bone were among the largest, as were those from the temporal bone, which also had the greatest variability. Those from the frontal, parietal, and zygomatic bones showed much overlap.

The differences within bones for each elastic modulus were most pronounced in the parietal, occipital, and temporal bones, while values within the frontal and zygomatic bones were more similar. For E_1, the most apparent difference was the large average modulus at T3 (15.0 GPa), which was greater than that of other zygoma sites. P1 (14.8 GPa) was also large compared to the sites with the lowest values in the parietal bone (P6: 12.2 GPa and P8: 12.3 GPa). For E_2, differences within bones were similar to those in E_1, especially regarding the large value for T3 (17.7 GPa), which was similar to that of the nearby occipital protuberance site (O2), but differed from other temporal bone sites. T1, T2, and T4 averaged 5 GPa less than T3, and were similar to E_2 values from the zygoma.

For E_3, the larger differences within bones were found in the parietal, occipital, and temporal bones. These differences were not similar to the differences within bones for E_1 and E_2, but corresponded with the presence or absence of an overlying muscle attachment. ANOVAs showed significant differences for E_3 between muscle-bearing and non-muscle-bearing sites, but not for E_1 and E_2 (Table 2). T4, a masseter attachment site on the zygomatic process of the temporal bone, was the stiffest of all sampled sites (27.3 GPa). Site P11, which was a muscle-bearing site for the posterior temporalis, was the stiffest site within the parietal bone. E_3 for P11 was similar to O3 and T2, which are also muscle attachment sites.

A scatterplot of mean values of E_2 vs. E_3 (Fig. 3) demonstrated the lack of correlation between the two variables, and showed that while most E_2 values group by bone, most E_3 values group by muscle attachment. Sites with muscle attachment had higher E_3 values and were represented by solid shapes, mostly on the right side of the plot.

Anisotropy within the plane of the cortical plate (E_2/E_3) (Table 2 and Fig. 4) showed significant differences between and within bones. This pattern did not follow that of either E_2 or E_3; rather, it was a combination of the two, representing unique differences between bones in anisotropy coupled with differences between muscle-bearing and non-muscle-bearing sites within some bones. However, anisotropy did not show a significant difference between muscle-bearing and non-muscle-bearing sites overall.

Anisotropy decreased as cortical thickness increased (Fig. 4). This relationship was significant for all individual specimens ($R = 0.50$, $P < 0.001$) as well as for mean values by site ($R = 0.75$, $P < 0.001$). Correlations of E_2 ($R = 0.30$, $P < 0.001$) and E_3 ($R = -0.25$, $P < 0.001$) individually with thickness were weaker, showing a slight increase in E_2 and a slight decline in E_3 in thicker cortical specimens.

Cortical samples from the zygoma were among the most anisotropic (lowest E_2/E_3 ratios) and showed the least variability between sites. The temporal bone also had highly anisotropic sites but also had the greatest variability between sites of all bones. The non-muscle-bearing site at T3, the occipitomastoid, had low anisotropy similar to that of adjacent occipital bone sites. The remaining temporal bone sites were muscle-bearing and showed some of

TABLE 2. Elastic moduli (GPa) and E_2/E_3 anisotropy

		E_1		E_2		E_3		E_2/E_3	
Bone	Site	Mean	SD	Mean	SD	Mean	SD	Mean	SD
Parietal	1	14.8	2.3	15.7	2.6	20.9	3.5	0.76	0.13
	2	13.9	2.5	15.4	3.8	20.0	3.9	0.78	0.17
	3	12.8	3.8	14.6	3.7	17.9	4.7	0.83	0.10
	4	13.4	2.4	15.2	3.1	18.7	4.1	0.83	0.14
	5	12.7	2.6	14.1	3.5	18.5	4.4	0.78	0.14
	6	12.2	3.0	12.3	3.3	20.7	3.8	0.60	0.15
	7	13.3	2.8	14.3	3.7	19.1	4.7	0.77	0.15
	8	12.3	2.7	12.4	2.9	20.1	4.3	0.63	0.17
	9	12.8	2.5	13.7	4.0	19.9	4.6	0.72	0.23
	10	13.6	3.0	14.8	3.6	20.6	3.7	0.72	0.12
	11	13.9	2.7	15.0	3.1	23.5	4.3	0.65	0.13
	12	12.8	3.5	13.1	4.2	21.5	4.8	0.62	0.20
	13	13.1	2.6	14.2	3.4	20.5	4.7	0.71	0.17
	14	12.4	3.5	12.3	4.1	22.2	5.6	0.57	0.18
Grand mean		13.1	2.9	14.1	3.6	20.3	4.5	0.71	0.17
Frontal	1	12.5	2.4	13.4	3.4	20.2	4.3	0.68	0.18
	2	12.9	1.9	15.0	2.6	19.6	4.0	0.78	0.14
	3	12.9	2.4	15.0	3.2	20.6	3.5	0.74	0.16
	4	12.5	2.8	13.4	3.1	19.5	4.0	0.69	0.13
	5	12.4	2.1	15.8	2.6	19.4	3.4	0.81	0.12
	6	13.1	2.1	15.9	3.4	19.6	4.5	0.82	0.12
	7	12.3	2.5	14.1	3.6	18.6	3.5	0.76	0.17
	8	12.0	3.1	13.7	3.8	19.5	5.3	0.73	0.19
	9	11.8	3.2	12.6	4.4	17.6	5.0	0.71	0.14
Grand mean		12.5	2.5	14.3	3.5	19.4	4.2	0.75	0.16
Occipital	1	12.6	2.2	14.3	2.6	17.9	3.7	0.81	0.13
	2	13.5	2.8	16.8	3.9	20.9	4.6	0.81	0.13
	3	14.1	1.9	16.1	3.1	22.5	3.6	0.72	0.14
	4	13.7	2.4	16.0	3.4	20.6	5.0	0.79	0.15
	5	13.6	2.5	16.0	3.4	20.9	5.5	0.80	0.17
Grand mean		13.5	2.4	15.8	3.3	20.6	4.7	0.79	0.15
Temporal	1	11.7	3.7	12.2	4.1	20.4	5.3	0.61	0.19
	2	12.8	3.6	12.8	4.8	24.1	3.7	0.54	0.20
	3	15.0	1.9	17.7	2.4	21.8	1.9	0.81	0.09
	4	14.1	2.3	13.3	2.2	27.3	6.0	0.51	0.16
Grand mean		13.4	3.2	14.0	4.1	23.4	5.1	0.62	0.20
Zygoma	1	10.2	2.3	12.1	3.1	19.2	5.9	0.67	0.20
	2	11.0	3.5	12.5	3.7	20.5	6.1	0.63	0.18
	3	10.4	3.2	11.7	3.7	19.1	3.4	0.62	0.20
	4	9.7	2.1	10.5	3.8	19.7	6.2	0.56	0.21
Grand mean		10.4	3.0	11.7	3.5	19.6	5.4	0.62	0.20
Grand mean	MBB[a]	12.5	2.6	13.6	4.0	21.2	5.3	0.66	0.19
Grand mean	Non-MBB	13.0	3.0	14.5	3.4	19.7	4.1	0.75	0.16
ANOVA		F	P	F	P	F	P	F	P
Bone		18.8	0.001	12.0	0.001	6.0	0.001	16.6	0.001
Site/bone		3.3	0.001	2.4	0.001	2.8	0.001	3.6	0.001
Muscle		4.1	NS	13.4	0.003	20.0	0.001	38.3	0.001

[a]MBB, muscle bearing bone.

the greatest anisotropy of all sites. The zygomatic process of the temporal bone had the greatest anisotropy (0.51) and the largest E_3 value of all sites. The parietal and frontal bones had large variability in anisotropy and muscle-bearing sites, and both bones tended to have the larger values. Of interest here is that, with the exception of P3, the most anisotropic of the non-muscle-bearing sites were closer to the temporal line and the origin of the temporalis muscle. The occipital bone had consistently low anisotropy, despite muscle attachments at four of five sites. The muscle-bearing sites had relatively large values of both E_2 and E_3, while the non-muscle-bearing site (O1) had a low mean E_3 value and an intermediate E_2 value.

There were significant differences for G_{12}, G_{13}, and G_{23} between bones, but not between sites within bones (Table 3). Site means of G_{13} (3.7–5.8 GPa) were larger than those of G_{12} (3.4–5.3 GPa), although the ranges extensively overlapped. Shear moduli G_{23} in the plane of the external cortex (5.5–7.5 GPa) were the largest. Overall, the smallest shear moduli were found in the zygoma, and the largest were in the temporal and occipital bones.

The Poisson's ratios (Table 4) showed significant differences between bones (except for V_{32}) and between sites within bones. Poisson's ratio is the ratio of the strain perpendicular to the applied load divided by the strain in the direction of the applied load, and is thus dependent on the three-dimensional elastic properties of the material. Variation for four of the ratios was similar to that described for other properties, in that the occipital bone was at one extreme as the largest (v_{13}, v_{23}) or the smallest (v_{12},

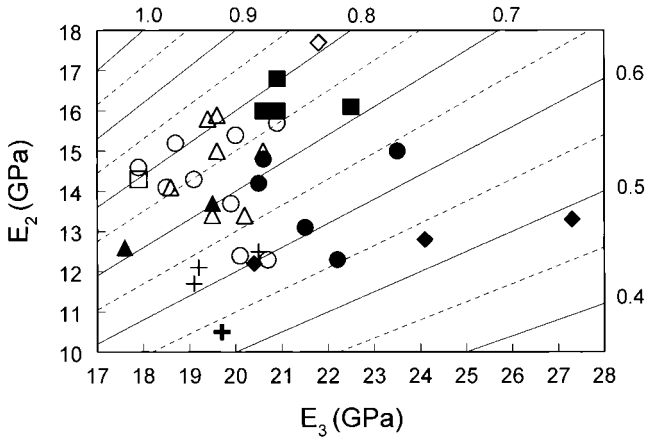

Fig. 3. Scatterplot of mean E_2 vs. mean E_3 showing the range of anisotropy for all sites. Note that the muscle bearing sites (bold and filled symbols) are primarily on the right side of the graph, while the nonmuscle bearing sites (light and hollow symbols) are primarily on the left side of the graph. E_2 is the elastic modulus in the direction of minimum stiffness, and E_3 is the elastic modulus in the direction of maximum stiffness. The numbers on the upper and left borders label the diagonal lines that indicate the E_2/E_3 anisotropy ratios. Symbols are the same as in Figure 2.

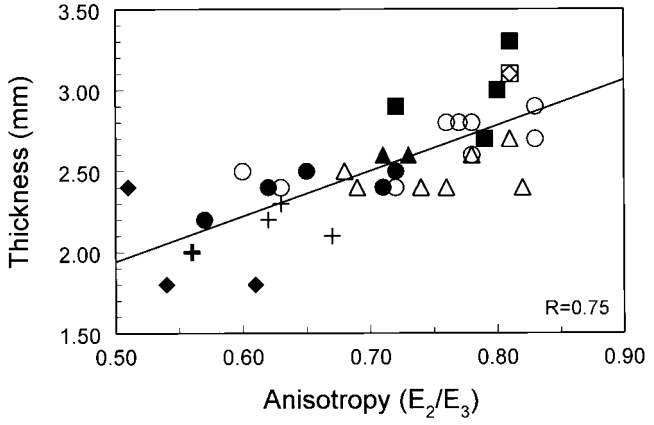

Fig. 4. Scatterplot of mean thickness vs. mean anisotropy showing muscle-bearing (M) sites as solid, and non-muscle-bearing (NM) sites as hollow. There is a significant relationship ($R = 0.75$, $P < 0.001$), indicating that as thickness increases so does anisotropy. Symbols are the same as in Figure 2.

v_{21}), the zygoma was at the other extreme, the parietal and frontal bones had intermediate values, and the temporal bone had values across much of the total range. Differences between bones were smaller than in other variables: v_{32} showed no significant differences between bones, and v_{31} had great overlap of the means among bones, as indicated by a low P-value (0.04). Within each bone, the occipital, frontal, and zygomatic bones tended to have similar values for all ratios. The temporalis showed a distinction between T3 and other sites for all ratios, except v_{32}. The parietal bone showed differences that reflected variation between muscle-bearing and non-muscle-bearing sites, especially v_{12}, v_{13}, v_{21}, v_{23}, but not v_{31} or v_{32}. Poisson's ratios were largest in the v_{21} and v_{12} directions, intermediate in the v_{31} and v_{32} directions, and smallest in the v_{13} and v_{23} directions.

Rayleigh's test for uniformity demonstrated significant mean directions of greatest stiffness in nine sites (Table 5, Fig. 5). Because of the variability of the angular dispersion, 27 sites did not show any significant mean direction. Since there was a significant difference in E_3 between muscle-bearing sites and non-muscle-bearing sites (Table 2), we tested whether muscle-bearing sites were more likely to have a significant mean direction of maximum stiffness. A 2×2 chi-square indicated no significant difference between muscle-bearing bone and non-muscle-bearing bone in the presence or absence of a significant orientation.

Despite the lack of an overall significant difference in orientation between muscle-bearing and non-muscle-bearing bone, there did appear to be a difference between them if only the oriented sites were considered. The significant mean direction of greatest stiffness at all muscle-bearing sites (T4, F9, P11, P12, and P13) was perpendicular to the direction of the muscle pull, while that of two non-muscle-bearing sites (P5 and P6) was parallel to the direction of muscle pull at the closest muscle-bearing sites.

Two sites on the frontal bone, which were anatomically more distant from masticatory muscle attachments, showed significant mean orientations of the axes of maximum stiffness. F1, the site at the glabella of the frontal bone, showed a significant direction of maximum stiffness parallel with the brow ridge. F3 was unusual among midline sites in that it had a mean direction of maximum stiffness roughly parallel to the sagittal suture.

DISCUSSION

Variation Between and Within Bones

Our results demonstrate patterns of variation in the material properties of the external cortex of the cranial vault and zygoma. For some variables, these patterns are correlated and relate to the bone or region of the skull from which the data are derived. For other variables, material properties demonstrate a pattern that has a functional correlate. These patterns can be summarized as follows:

1. Cortical thickness, density, E_1, E_2, all shear moduli, v_{13}, v_{23}, and E_2/E_3 anisotropy vary together by bone and generally are greater for the occipital bone, intermediate for the frontal and parietal bones, and least for the zygoma. v_{12} and v_{21} are in a similar but reverse order, from smallest to largest mean values by bone. The temporal bone has a wider range of values for most variables, and does not have a consistent place in this order.

2. Although E_3 shows some differences between bones, these are less clear and do not correspond to those of the other variables. Our results show that most-muscle bearing sites are stiffer along the axis of maximum stiffness than are non-muscle-bearing sites.

3. v_{31} and v_{32} showed fewer differences between bones and sites within bones than other variables. They showed no discernable pattern relating to location or function.

Some unusual features were observed within individual bones. In particular, sites T3 and Z2 resembled adjacent sites in other bones. The thickness and density of Z2, the site on the frontal process of the zygoma, were similar to many sites on the cranial vault. This may relate to the functional similarity of site Z2 to adjacent portions of the

TABLE 3. Shear moduli (GPa)

		G_{12}		G_{13}		G_{23}	
Bone	Site	Mean	SD	Mean	SD	Mean	SD
Parietal	1	5.2	0.9	5.5	0.8	7.3	1.1
	2	4.8	1.0	5.1	0.8	7.2	1.4
	3	4.5	1.1	4.7	1.3	6.6	1.9
	4	4.7	0.9	4.9	1.0	6.6	1.1
	5	4.5	1.0	5.0	1.1	6.5	1.3
	6	4.1	0.9	4.7	1.0	6.6	1.2
	7	4.6	1.0	5.2	1.1	6.6	1.5
	8	4.4	0.8	4.7	0.9	6.4	1.0
	9	4.7	0.9	5.2	0.8	6.7	1.0
	10	4.6	1.2	5.0	1.2	6.7	1.6
	11	4.6	1.0	5.2	1.0	7.1	1.1
	12	4.6	0.8	5.4	1.1	6.9	1.3
	13	4.6	0.9	5.3	1.0	6.9	1.5
	14	4.4	1.0	5.0	1.2	6.9	1.5
Grand mean		4.6	1.0	5.1	1.0	6.8	1.3
Frontal	1	4.4	1.0	5.1	1.1	6.5	1.0
	2	4.4	0.9	4.5	0.8	6.6	0.7
	3	4.4	1.1	4.9	1.2	6.9	1.0
	4	4.3	0.9	4.8	1.2	6.5	1.1
	5	4.2	0.9	4.5	1.0	6.4	1.0
	6	4.4	0.7	4.7	0.9	6.6	1.1
	7	4.3	1.1	4.5	0.8	6.3	1.2
	8	4.0	1.1	4.4	1.3	6.1	1.4
	9	4.2	1.3	4.6	1.3	6.1	1.4
Grand mean		4.3	1.0	4.6	1.1	6.4	1.1
Occipital	1	4.5	1.0	4.7	1.2	6.4	1.0
	2	5.1	1.1	5.4	1.0	7.0	1.5
	3	4.8	0.8	5.4	0.8	7.5	0.9
	4	4.9	0.9	5.1	1.3	6.9	1.2
	5	5.1	1.1	5.7	1.2	7.3	1.3
Grand mean		4.9	1.0	5.2	1.1	7.0	1.2
Temporal	1	4.3	0.9	4.6	0.9	6.9	1.3
	2	4.4	0.9	4.9	0.9	7.2	1.2
	3	5.3	0.8	5.6	0.7	7.3	0.9
	4	5.0	0.7	5.8	0.8	7.2	0.9
Grand mean		4.7	1.0	5.3	1.0	7.1	1.1
Zygoma	1	3.6	0.7	4.1	1.4	5.8	1.2
	2	3.9	1.4	4.5	1.1	6.4	1.4
	3	3.7	1.1	4.1	1.0	5.7	1.1
	4	3.4	1.0	3.7	0.1	5.5	1.4
Grand mean		3.7	1.1	4.1	1.1	5.8	1.3
Grand mean	MBB	4.4	1.1	4.9	1.2	6.7	1.4
Grand mean	Non-MBB	4.5	1.0	4.9	1.0	6.7	1.2
ANOVA		F	P	F	P	F	P
Bone		30.1	0.001	31.2	0.001	10.6	0.001
Site/bone		1.7	NS	2.4	NS	2.3	NS
Muscle	MBB	2.0	NS	0.08	NS	0.05	NS

frontal bone forming the supra- and lateral-orbital regions.

Compared to the parietal and frontal bones, zygoma sites (other than Z2) have lower thickness and density. The mechanical significance of this may relate to the unique structure of the zygoma. The zygoma has a relatively dense core of trabecular bone, which may play a more significant structural role than the proportionately lesser amounts of trabecular bone in most other craniofacial bones.

Temporal bone sites show the largest variation in material properties of all the cranial vault bones. T3, the most posterior site on the temporal bone, resemble certain aspects of the adjacent occipital bone, while sites T1 and T2 resemble aspects of adjacent parietal bone sites. T4, the site on the zygomatic process of the temporal bone, has the largest E_3 and anisotropy of all cranial sites.

Differences found in the temporal bone correspond with the functional and developmental differences in portions of the bone. The four sites arise from two different developmental regions, including the mastoid portion (T3), and the squamous portion (T1, T2, and T4). Within the squamous portion, T1 and T2 are from a region of the cranial vault that lacks a diploë. Vault thickness at these sites is thus the full thickness of the vault. Thickness in this region is thinner than the external cortex alone at all other vault sites, but density and most elastic properties are similar to those of other bones, especially the frontal and parietal bones. The thinner bone in the squamous portion of the temporal bone may imply a reduced struc-

TABLE 4. Poisson's ratios

		V_{12}		V_{13}		V_{21}		V_{23}		V_{31}		V_{32}	
Bone	Site	Mean	SD	Mean	SD	Mean	SD	Mean	SD	Mean	SD	Mean	SD
Parietal	1	0.46	0.12	0.22	0.07	0.48	0.08	0.24	0.08	0.30	0.08	0.31	0.06
	2	0.44	0.16	0.25	0.09	0.46	0.11	0.23	0.07	0.35	0.11	0.30	0.05
	3	0.43	0.08	0.25	0.07	0.48	0.07	0.27	0.07	0.34	0.08	0.32	0.06
	4	0.40	0.10	0.26	0.08	0.45	0.08	0.25	0.07	0.36	0.08	0.30	0.06
	5	0.42	0.09	0.26	0.08	0.46	0.09	0.27	0.08	0.37	0.06	0.34	0.07
	6	0.53	0.14	0.19	0.07	0.51	0.08	0.20	0.05	0.31	0.08	0.34	0.06
	7	0.43	0.12	0.26	0.07	0.45	0.08	0.26	0.07	0.37	0.08	0.34	0.05
	8	0.54	0.15	0.18	0.08	0.54	0.10	0.21	0.08	0.28	0.08	0.32	0.06
	9	0.50	0.22	0.21	0.11	0.49	0.11	0.24	0.09	0.31	0.14	0.34	0.08
	10	0.45	0.09	0.22	0.04	0.48	0.08	0.22	0.05	0.33	0.05	0.30	0.05
	11	0.48	0.13	0.19	0.07	0.52	0.09	0.18	0.06	0.31	0.08	0.27	0.05
	12	0.52	0.24	0.21	0.12	0.48	0.11	0.22	0.07	0.31	0.18	0.39	0.13
	13	0.44	0.16	0.25	0.09	0.45	0.07	0.25	0.06	0.37	0.11	0.35	0.06
	14	0.60	0.23	0.18	0.08	0.55	0.07	0.19	0.05	0.30	0.12	0.38	0.20
Grand mean		0.47	0.16	0.22	0.08	0.48	0.09	0.23	0.08	0.33	0.10	0.33	0.09
Frontal	1	0.49	0.16	0.19	0.10	0.50	0.10	0.22	0.12	0.30	0.14	0.31	0.11
	2	0.38	0.11	0.26	0.08	0.42	0.10	0.24	0.06	0.38	0.09	0.30	0.06
	3	0.42	0.15	0.24	0.08	0.46	0.11	0.22	0.07	0.37	0.08	0.30	0.07
	4	0.47	0.10	0.21	0.08	0.51	0.12	0.24	0.06	0.32	0.12	0.35	0.11
	5	0.36	0.08	0.26	0.05	0.45	0.08	0.24	0.06	0.41	0.05	0.30	0.04
	6	0.40	0.09	0.24	0.05	0.48	0.07	0.24	0.06	0.36	0.06	0.29	0.06
	7	0.43	0.15	0.21	0.08	0.47	0.12	0.23	0.07	0.32	0.12	0.30	0.06
	8	0.46	0.14	0.22	0.10	0.51	0.12	0.22	0.09	0.34	0.12	0.29	0.07
	9	0.47	0.16	0.20	0.11	0.49	0.13	0.26	0.08	0.30	0.17	0.38	0.12
Grand mean		0.43	0.14	0.23	0.09	0.48	0.11	0.24	0.10	0.34	0.11	0.31	0.08
Occipital	1	0.38	0.10	0.28	0.09	0.43	0.11	0.28	0.08	0.39	0.10	0.34	0.08
	2	0.35	0.10	0.26	0.07	0.41	0.10	0.26	0.06	0.35	0.09	0.31	0.05
	3	0.40	0.12	0.24	0.08	0.44	0.09	0.22	0.07	0.37	0.09	0.30	0.05
	4	0.45	0.11	0.20	0.08	0.50	0.06	0.24	0.11	0.30	0.12	0.30	0.11
	5	0.39	0.13	0.24	0.10	0.44	0.10	0.28	0.10	0.33	0.13	0.34	0.08
Grand mean		0.40	0.12	0.24	0.09	0.45	0.09	0.26	0.10	0.35	0.11	0.32	0.08
Temporal	1	0.57	0.18	0.18	0.09	0.54	0.11	0.21	0.09	0.29	0.12	0.36	0.09
	2	0.62	0.21	0.14	0.09	0.57	0.12	0.16	0.06	0.24	0.12	0.30	0.06
	3	0.35	0.06	0.27	0.05	0.41	0.08	0.26	0.05	0.38	0.06	0.32	0.04
	4	0.52	0.15	0.16	0.11	0.48	0.12	0.17	0.10	0.27	0.11	0.31	0.09
Grand mean		0.52	0.19	0.19	0.09	0.50	0.12	0.20	0.09	0.30	0.11	0.32	0.07
Zygoma	1	0.44	0.22	0.21	0.11	0.48	0.16	0.22	0.10	0.36	0.19	0.32	0.10
	2	0.44	0.16	0.21	0.09	0.50	0.16	0.22	0.10	0.38	0.14	0.34	0.11
	3	0.46	0.20	0.20	0.09	0.47	0.12	0.19	0.06	0.34	0.18	0.31	0.09
	4	0.56	0.16	0.16	0.10	0.56	0.09	0.17	0.09	0.29	0.15	0.31	0.10
Grand mean		0.48	0.19	0.19	0.10	0.50	0.13	0.20	0.10	0.35	0.17	0.32	0.10
MBB		0.48	0.18	0.20	0.10	0.49	0.11	0.24	0.08	0.32	0.13	0.32	0.10
Non-MBB		0.43	0.13	0.23	0.08	0.47	0.10	0.21	0.08	0.34	0.10	0.33	0.07
ANOVA		F	P	F	P	F	P	F	P	F	P	F	P
Bone		8.3	0.001	5.4	0.001	4.1	0.003	7.4	0.001	2.6	0.036	0.7	NS
Site/bone		2.8	0.001	2.2	0.001	2.3	0.001	2.0	0.002	1.7	0.011	1.9	0.003
Muscle		13.2	0.001	15.3	0.001	4.9	0.030	16.3	0.001	5.3	0.020	1.1	NS

tural role; however, this is unclear because the vault in general is overbuilt for resisting loads engendered by oral functions.

The remaining site from the squamous portion of the temporal bone, T4, is located on the zygomatic process and does not make up part of the cranial vault. This site is unique among those studied in having the highest values of E_3. This large maximum stiffness, coupled with an intermediate E_2 value, also gives this site the greatest anisotropy. These properties may correspond with functional features of the posterior zygomatic arch. T4 is muscle-bearing, and the masseter attaches to a relatively small surface area of the bone in this region compared to the larger attachment areas for the temporalis and nuchal musculature. Also, the masseter in this region is relatively

TABLE 5. Direction of greatest stiffness by degrees

		Mean vector	Circular CI	Rayleigh's test of uniformity[a]
Bone	Site	Mean °	95% CI	*P* value
Parietal	5	103	15	0.01
	6	79	18	0.01
	11	26	17	0.01
	12	5	18	0.01
	13	26	20	0.02
Frontal	1	76	20	0.02
	3	10	13	0.01
	9	38	21	0.04
Temporal	4	25	8	0.01

[a]Oriana indicated the above sites as significant using Rayleigh's test of uniformity or test of significance.

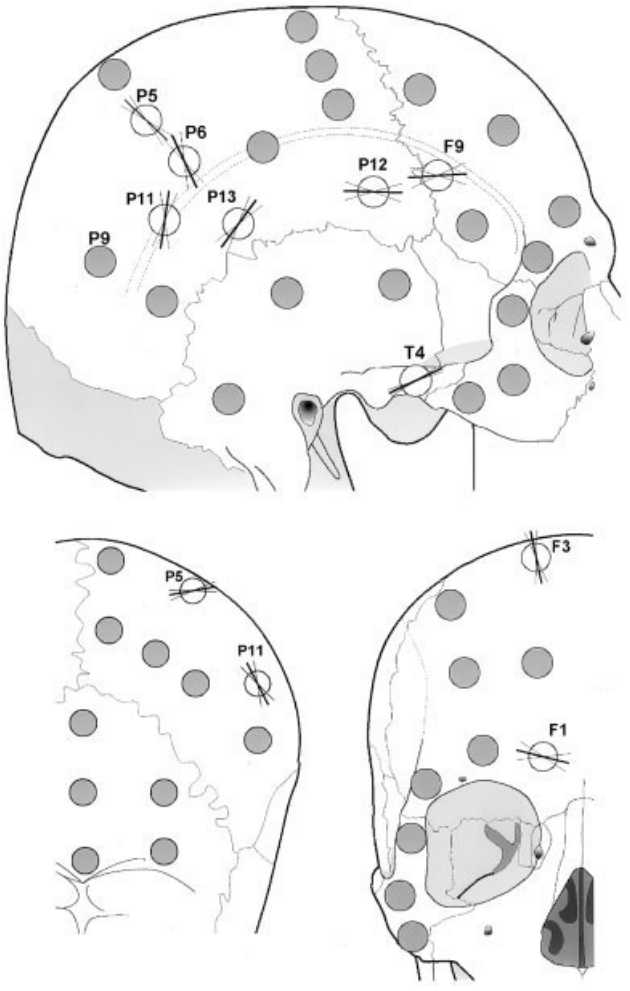

Fig. 5. Orientation of axes of maximum stiffness in the frontal, sagittal, and occipital views. Nine sites show a significant mean orientation of maximum stiffness, as indicated by the central line at each significant site. Error is indicated by lines for the 95% CIs. All shaded sites have no significant mean maximum direction of stiffness.

less complex than the temporalis or nuchal musculature, suggesting less variation in the direction of loading during multiple functional activities. The large E_3 at this site corresponds with the larger E_3 values found at all muscle-bearing sites. We hypothesize that the large anisotropy and invariant orientation of the axis of maximum stiffness relates to a common pattern of stress orientation, which results from the local effects of masseter contraction during oral activities.

Occipital bone sites O2–O5 have unique features, including some of the thickest cortical bone in the skull. The distinct material properties of the occipital bone may relate to its functional role as an attachment area for the nuchal musculature, which functions in head posturing and movement. This musculature differs from the masticatory muscles in several ways. The nuchal musculature pulls against the bone at a less acute angle. For example, the temporalis pulls against the parietal and temporal bones at an angle nearly parallel to the bone surface. Also, the nuchal musculature is comprised of several complex muscles that are generally thicker and stronger than the muscles of mastication. Whether the angle and magnitude of muscle pull generally relate to cortical bone thickness and elastic properties is an interesting question that requires further study.

Some aspects of our current results are similar to those in a previous study, in which we examined differences between the inner and outer tables of the parietal bone (Peterson and Dechow, 2002). However, in the previous study a smaller sample size was used, and some specimens were rehydrated from dry skulls. Elastic properties of the outer cortical plate were very similar between the two studies; however, the previous investigation showed fewer significant differences between sites within the external cortex, which is likely an effect of the smaller sample sizes in the previous study. The largest difference between the studies was a smaller mean for the thickness of the external cortical plate (1.8 mm vs. 2.5 mm). We suspect that this difference is due to demographic differences in age and dental condition. All samples in the current investigation came from dentate individuals of known age. These details were not available for samples in our earlier study; however, unless an effort is made to specifically collect samples from dentate individuals, most cadaver material comes from edentulous or partially dentate individuals.

Anisotropy and Orientation

The values of elastic moduli illustrate an order ($E_3 > E_2 \geq E_1$, and $G_{32} > G_{31} \geq G_{12}$) that indicates transverse isotropy, as found in the diaphyses of long bones (Yoon and Katz, 1976; Ashman, 1989; Rho, 1996). The average anisotropies of the zygoma are lower in magnitude than the other bones tested in this study, but are similar to the parietal bone inner table cortical elastic properties (Peterson and Dechow, 2002). The similarity in anisotropies among cranial bone specimens from most sites and similar measurements taken from postcranial specimens (Ashman, 1989) suggests similarities in the three dimensional aspects of their microstructure. If function and bone microstructure are related, then a reasonable hypothesis for further study is that the relative lack of strain in the cranial vault results in the lack of consistent material orientation.

One surprising finding was that the elastic properties of the cranial vault are more similar to those measured in long bones of the postcranial skeleton than to those of the mandible (Ashman, 1989; Dechow and Hylander, 2000; Schwartz-Dabney and Dechow, 2003). The main difference between the mandible and the cranial vault is the relatively high values of E_2 in the mandible. On average, E_2 is only slightly greater than E_1 in the cranial vault, indicating transverse isotropy. However, in the mandible, E_2 is often equidistant between E_1 and E_3 in magnitude, indicating orthotropy. There is considerable variation in these features between sites in both the cranial vault and the mandible, which indicates that these differences cannot be ascribed strictly to location or pattern of development. We suspect that an explanation of these differences will require more specific knowledge of mechanical microenvironments, local influences (such as muscle attachment on bone strain), and an understanding of the three-dimensional nature of bone structure and adaptation.

Unfortunately, we know little about the three-dimensional intermediate structure of cranial cortical bone. The

only attempts to understand patterns of osteonal orientation and microstructure in the cranial vault are found in historic studies of split-lines, which do not provide sufficient information to adequately describe this intermediate cortical structure. In split-line studies of the periosteal surface of decalcified bone, investigators have attempted to outline functional anatomical regions defined by the orientation or "grain" of bone (Benninghoff, 1925). Split-lines likely reflect aspects of bone histology, including Haversian system anatomy and vascular canal orientation (Seipel, 1948; Tappen, 1954, 1967; Dempster and Coleman, 1960; Buckland-Wright, 1977). However, it is unlikely that, as suggested by Dempster and Coleman (1960), split-lines show the orientation of collagenous fibers and inorganic crystallites.

One problem that arose when we attempted to compare our directions of maximum stiffness with split-line orientations is that previous studies did not document variability in split-lines quantitatively. In the mandible, we found that split-lines on the whole corresponded with directions of maximum stiffness (Schwartz-Dabney and Dechow, 2003). In the cranium and facial skeletons, correspondence between the two was at best sporadic. Tappen (1964) observed split-lines in areas where the loads produced by muscle forces acting on the bone must be principally tensile. We found sites that support muscle attachment (F9, P11, P12, P13, and T4) to be significantly anisotropic and have a significant mean direction of stiffness similar to split-line orientation described by Tappen. We also found a significant mean direction of stiffness at one site near a bony suture (F3), where forces may be tensile (Mooney et al., 1998). However, other muscle-bearing sites and sites adjacent to sutures had no significant mean orientation between individuals, which calls into question the meaning of any such similarities.

Other studies of split-lines likewise show a lack of correspondence with our results. The split-line pattern described by Benninghoff (1934) in the parietal region showed crescent-shaped lines parallel to the temporal line. This is similar to our findings regarding the orientation of maximum stiffness at some sites, but differs for most sites. Dempster (1965) described cranial vault split-line patterns, and suggested that the grain of the cranial external cortex follows the shape of the bony structures in the human skull. He demonstrated a split-line pattern unlike those described by Benninghoff (1925), Ahrens (1936), and Tappen (1954, 1957), yet different from our findings on directions of maximum stiffness. We did not find a mean direction of maximum stiffness at all sites, and did not see any patterns that related to the shape of the cortex.

Seipel (1948), in a study of split-lines in the craniofacial skeleton, discussed the "closed kinetic chains within the facial skeleton," including the frontal and temporal regions, which he noted serve the purposes of muscle insertion and skeletal stabilization. Seipel also discussed the direct muscular connections in the zygoma, which creates the closed kinetic chains. He argued that function is a determinant of the facial bony architecture and directions of "grain," as determined by split-lines, within the bone. However, while function may be an important determinant of the orientation of the principal axes of stiffness in the cortical bone of the skull, this relationship is not illuminated by historical data on split-lines.

Functional Implications

While it is possible that material properties correlate with regional stress patterns, this relationship is not clear. Skedros et al. (1994) examined artiodactyl calcanei to determine whether regional differences in strain magnitude and mode (tension vs. compression) reflect regional adaptations in the structural/material organization of bone. Their results were similar to ours in that they found regional differences in material properties, which may relate to differences in strain mode between specific skeletal locations and functions. For instance, they noted the differences in the cortical thickness of bone in regions of net tension vs. net compression in calcanei. The regional variations we observed in density, thickness, elastic modulus, anisotropy, and direction of greatest stiffness, and especially the differences between muscle-bearing and non-muscle-bearing sites in stiffness (see below), indicate the possibility of mechanically mediated adaptation.

Gradients of bone strain have been found by in vitro testing of human skulls (Endo, 1966, 1970), and by in vivo studies of the circumorbital region and zygomatic arch in rhesus monkeys and baboons (Hylander, 1987). Along the zygomatic arch, bone strains are higher in the anterior part of the arch and the temporal process of the zygoma than in the posterior part of the arch or the zygomatic process of the temporal bone. Specifically, we expected that this functional difference, which relates to attachments of the masseter muscle, would result in differences in elastic properties in that greater stiffness or more consistent orientation of the axes of stiffness might be found in the anterior part of the arch compared to the posterior part. However, the only site that showed a significant mean direction of stiffness across multiple samples was T4, which is on the zygomatic process of the temporal bone. The four sites on the zygoma, and the three on the squamosal portion of the temporal bone showed no significant directionality. T4 also had the largest value of E_3. These differences between T4 and nearby sites suggest functional implications, but this is difficult to interpret with our current knowledge regarding loading in this region and bone adaptation. One possibility is that loading patterns are more consistent in the posterior arch both within and between individuals, which results in less variability in patterns of bone remodeling and the related cortical material properties.

Cowin and Hart (1990) demonstrated a theoretical maximum error of 45° in principal stress axis orientation if anisotropic bone is modeled as isotropic. Dechow and Hylander (2000) extended these concepts empirically in the craniofacial skeleton, and showed how the variation in material anisotropy and direction of maximum stiffness contributes to errors in stress magnitudes and orientations calculated from experimentally measured bone strains. They concluded that regions of cortical bone with greater anisotropy and greater variation in the direction of maximum stiffness result in larger errors in calculating minimum and maximum stresses from bone strain. In the mandible, most regions have sufficiently consistent orientations of maximum stiffness to allow reasonable predictions of minimum and maximum stresses and their orientations. In the cranial vault, however, large errors may result at many sites if average values between subjects are used to make calculations of stress patterns in indi-

vidual bones. Stress in some parts of the cranial vault and zygoma can be more reliably calculated than in other regions, but this must be determined by analysis of the variation in the elastic properties, as discussed by Schwartz-Dabney and Dechow (2003).

When interpreting the results of this study, one must consider that the data are derived solely from the outer cortical table of the cranial vault, and do not include the inner cortical table or the diploic bone. The cranial vault functions as a three-layered structure, and additional studies incorporating all parts of the vault may provide additional insights into variations in cortical bone structure. A recent study in our laboratory showed material differences between the inner and outer tables in the parietal bone (Peterson and Dechow, 2002).

Our results differ from those of Dechow et al. (1993) in the supraorbit, in which the maximum direction of stiffness is not determined, but rather elastic coefficients are calculated based on anatomical landmarks. Given the variation in the maximum direction of stiffness, it is easy to see how Dechow et al. (1993) concluded that there is little difference at the supraorbit between E_2 and E_3. The direction of maximum stiffness throughout the cortex of the cranial vault and zygoma suggests the importance of measuring material orientation in cortical bone prior to determining material properties by ultrasonic or mechanical methods. We found a significant mean direction of stiffness for only nine of 36 sites in three of the five bones, and most of these nine sites showed variation between individuals. Only site T4 on the posterior zygomatic arch had great consistency in orientation among all samples. We did not find a mean direction of stiffness for the supraorbital site used by Dechow et al. (1993).

Despite the relatively great cortical thickness in the human cranial vault, and the presumed low strains, our results strongly indicate that the presence or absence of muscle attachment has an influence on elastic properties of the underlying cortical bone. T4, which had the largest E_3 of all sites, is loaded by the masseter and differs morphologically from other muscle-bearing sites on the cranial vault. However, the other muscle-bearing sites also show larger values of E_3, which indicates that muscle-bearing sites adapt to local strain microenvironments in which there is increased surface loading by increasing in maximum stiffness. There is also an effect on E_2 and thus in all directions within the plane of the cortical plate, although this effect is less pronounced than that for E_3. Likewise, E_2/E_3 anisotropy, like E_2 and E_3 (Fig. 3), differs between muscle-bearing and non-muscle-bearing regions. Most of this difference is attributable to E_3, and muscle-bearing cortical bone tends to have greater anisotropy. For instance, T4 has the greatest anisotropy of all sites.

Variation in the consistency of the orientation of the principal axes between sites may imply that a functional explanation for axis orientation is not sufficient. At some sites, the orientation of maximum stiffness in muscle-bearing bone is perpendicular to the orientation of muscle fibers and thus to muscle force. However, many muscle-bearing sites do not have a consistent orientation among individuals. Nevertheless, it is reasonable to hypothesize that muscle has a functional effect on bone elasticity. Additional research describing individual variations and ranges of variations in muscle function relative to material properties of specific adjacent cortical bone sites may show whether the direction of muscle pull is related to the direction of maximum stiffness in the underlying bone.

LITERATURE CITED

Ahrens HJ. 1936. Die Entwicklung der Spaltlineinarchitektur des knochernen menschlichen Schadels. Morph Jahrb 77:357–371.

Ashman RB. 1982. Ultrasonic determination of the elastic properties of cortical bone: techniques and limitations. Ph.D. dissertation, Tulane University, New Orleans, LA. U.M.I. Dissertation Services #8311363.

Ashman RB, Cowin SC, Van Buskirk WC, Rice JC. 1984. A continuous wave technique for measurement of the elastic properties of cortical bone. J Biomech 17:349–361.

Ashman RB, Van Buskirk WC. 1987. The elastic properties of a human mandible. Adv Dent Res 1:64–67.

Ashman RB. 1989. Experimental techniques. In: Cowin SC, editor. Bone mechanics. Boca Raton, FL: CRC Press, Inc. p 76–95.

Behrents RG, Carlson DS, Abdelnour T. 1978. In vivo analysis of bone strain about the sagittal suture in *Macaca mulatta* during masticatory movements. J Dent Res 57:904–908.

Benninghoff A. 1925. Spaltlinien am knochen, eine methode zur ermittlung der architektur platter knochen. Verh Anat Ges 34:189–206.

Benninghoff A. 1934. Die architektur der kiefer and ihrer weichteibedeckungen. Paradentium 6:2–20.

Buckland-Wright JC. 1977. Microradiographic and histological examination of the split-line formation in bone. J Anat 124:193–203.

Cowin SC, Hart RT. 1990. Errors in the orientation of the principal stress axes if bone tissue is modeled as isotropic. J Biomech 23:349–352.

Dechow PC, Nail GA, Schwartz-Dabney CL, Ashman RB. 1993. Elastic properties of human supraorbital and mandibular bone. Am J Phys Anthropol 90:291–306.

Dechow PC, Huynh T. 1994. Elastic properties and biomechanics of the baboon mandible (abstract). Am J Phys Anthropol 22:94–95.

Dechow PC, Hylander WL. 2000. Elastic properties and masticatory bone stress in the macaque mandible. Am J Phys Anthropol 112: 553–574.

Dempster WT, Coleman R. 1960. Tensile strength of bone along and across the grain. J Appl Physiol 16:355–360.

Dempster WT. 1965. The grain of cortical bone in relation to structural features of the adult skull. Anat Rec 151:342–343.

Endo B. 1966. Experimental studies on the mechanical significance of the form of the human facial skeleton. J Faculty Sci Univ Tokyo III:1–101.

Endo B. 1970. Analysis of stresses around the orbit due to masseter and temporalis muscles respectively. Am J Anthropol Soc Nippon 78:251–266.

Evans F, Lissner H. 1957. Tensile and compressive strength of human parietal bone. J Appl Physiol 10:493–497.

Evans F. 1973. Preservation effects. In: Evans F, editor. Mechanical properties of bone. Springfield: Charles C. Thomas. p 56–60.

Fisher NI. 1993. Statistical analysis of circular data. Cambridge, UK: Cambridge University Press. 277 p.

Hylander WL. 1987. Loading patterns and jaw movements during mastication in *Macaca fascicularis*: a bone-strain, electromyographic, and cineradiographic analysis. Am J Phys Anthropol 72: 287–314.

Mooney MP, Siegel MI, Burrows AM, Smith TD, Losken HW, Dechant J, Cooper G, Fellows-Mayle W, Kapucu MR, Kapucu LO. 1998. A rabbit model of human familial, nonsyndromic unicoronal suture synostosis. II. Intracranial contents, intracranial volume, and intracranial pressure. Childs Nerv Syst 14:247–255.

Peterson J, Dechow P. 2002. Differing material properties of the human parietal inner and outer cortical tables. Anat Rec 268:7–15.

Ravosa M, Noble V, Hylander WL, Johnson K, Kowalski E. 2000. Masticatory stress, orbital orientation and the evolution of the primate postorbital bar. J Hum Evol 83:667–693.

Rho JY. 1996. An ultrasonic method for measuring the elastic properties of human tibial cortical and cancellous bone. Ultrasonics 34:777.

Schröder WG, von dem Berge W, Lippert H. 1977. Biomechanik des Schadeldachs. Unfallheilkunde 80:391–395.

Schwartz-Dabney CL, Dechow PC. 2002. Accuracy of elastic property measurement in mandibular cortical bone is improved by using cylindrical specimens. J Biomech Eng 124:714–723.

Schwartz-Dabney CL, Dechow PC. 2003. Variations in cortical material properties throughout the human dentate mandible. Am J Phys Anthropol 120:252–277.

Seipel CM. 1948. Trajectories of the jaws. Acta Odontol Scand 8:81–191.

Sicher H, DuBrul EL. 1970. Oral anatomy. 5th ed. St. Louis, MO: C.V. Mosby Company. 502 p.

Skedros J, Mason M, Bloebaum R. 1994. Differences in osteonal micromorphology between tensile and compressive cortices of a bending skeletal system: indications of potential strain-specific differences in bone microstructure. Anat Rec 239:405–413.

Tappen N. 1954. A comparative functional analysis of primate skulls by the split-line technique. Hum Biol 26:220–238.

Tappen N. 1957. A comparison of split-line patterns in the skulls of a juvenile and an adult male gorilla. Am J Phys Anthropol 15:49–57.

Tappen N. 1964. An examination of alternative explanations of split-line orientation in compact bone. Am J Phys Anthropol 22:423–442.

Tappen NC. 1967. Some relationships between split-line patterns and underlying structure in primate skeletons. In: Starck DR, Schneider R, Kuhn H-J, editors. Neue Ergebnisse der Primatologie (Progress in primatology). Stuttgart: Gustav Fischer Verlag. p 80–89.

Yoon HS, Katz JL. 1976. Ultrasonic wave propagation in human cortical bone—II. Measurements of elastic properties and microhardness. J Biomech 9:459–464.

Zioupos P, Smith CW, An YH. 2000. Factors affecting mechanical properties of bone. In: An YH, Draughn RA, editors. Mechanical testing of bone and the bone-implant interface. Boca Raton, FL: CRC Press. p 87–101.